CHALMERS
UNIVERSITY OF TECHNOLOGY

3D-Printed Silver-Coated Vivaldi Array with Integrated Coaxial Probe Feeding

Citation for the original published paper (version of record):
Ayebe, M., Maaskant, R., Malmstrom, J. et al (2024). 3D-Printed Silver-Coated Vivaldi Array with Integrated Coaxial Probe Feeding. IEEE Antennas and Propagation Society, AP-S International Symposium (Digest): 7-8. http://dx.doi.org/10.1109/AP-S/INC-USNC-URSI52054.2024.10686495

(article starts on next page)

3D-printed Silver-coated Vivaldi Array With Integrated Coaxial Probe Feeding

Mustafa Ayebe[(1)], Rob Maaskant[(1)], Johan Malmström[(2)], Sten E. Gunnarson[(2)], Henrik Holter[(3)], and Marianna Ivashina[(1)]

[(1)] Chalmers University of Technology, Göteborg, Sweden
[(2)] SAAB, Järfälla, Sweden
[(3)] Ericsson AB, Stockholm, Sweden

***Abstract*—A Vivaldi antenna array is designed for large phased array applications in the 3–6 GHz frequency range and is fed by a novel coaxial probe through the ground plane. The simulated infinite array active reflection coefficient is below -10 dB for an up to $\pm 60^\circ$ scan in the E-plane and $\pm 50^\circ$ in the H-plane, across the entire frequency range. The measured active reflection coefficient and array pattern for a small-scale 1×5 Vivaldi array are in good agreement with the simulations, which validate the infinite array model including the probe feeding concept. Furthermore, the 3D printing and silver-coating fabrication process proves useful for rapid and cost-effective prototyping.**

I. Introduction

Phased arrays that are used in radar, sensor, and communication applications, enable electronic beam steering, offer multi-beam operation, flexible radiation pattern shaping, and are capable of mitigating interference signals. Particularly, when wide-band wide-angle centimeter frequency applications are considered, e.g. numerous 5G communication, radar, and imaging systems, Vivaldi antennas are often considered as promising candidates [1].

Traditional manufacturing of 3-D arrays involves the complex assembly of individually manufactured planar antenna elements or tiles, realized in PCB or metal technologies. This process requires precision in both mechanical alignment and electrical connectivity, leading to increased costs. Emerging technologies, such as 3D printing, may offer cost-effective alternatives by simplifying the manufacturing and assembly processes for Vivaldi antenna arrays [2].

This paper introduces a linearly polarized Vivaldi antenna array for dense phased-array applications in the 3–6 GHz band. Each antenna element is fed by a commercial coaxial probe that directly interfaces to an SMA connector[1]. The optimized infinite array design is validated for a small-scale 1×5 Vivaldi array by comparing simulations to measurements.

Finally, we also explore the potential of resin additive-manufactured (AM) antennas that are subsequently silver-coated. This is motivated by the suitability of AM techniques of metal structures and in constructing complex geometric models. A noteworthy illustration is provided in [3], where a 3-D Vivaldi antenna for ultra-wideband (UWB) applications is designed and manufactured using AM technology, showcasing the versatility of this approach.

[1]Amphenol SV Microwave, SF2950-6200

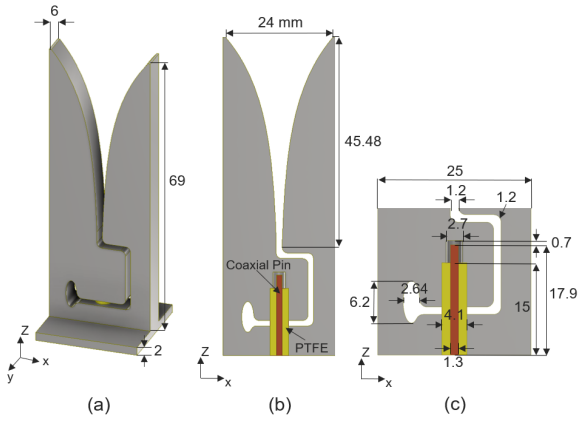

Fig. 1. Simulated geometrical model with dimensions in millimeters. (a) 3D view of the unit-cell model; (b) Cross-section of the antenna element in the x-z plane, and; (c) Detailed view of the feeding section.

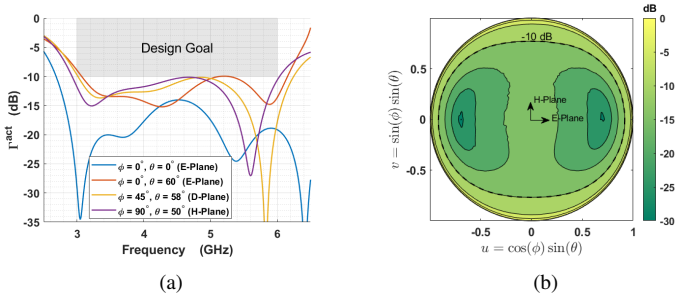

Fig. 2. Infinite array active reflection coefficient: (a) at various steering angles versus frequency; (b) in all planes at 4.5 GHz as a function of steering angle.

II. Antenna Structure and Simulation

1) Antenna Element Structure: The Vivaldi element, constructed from a single 3D printed and metalized part, is fed using a $50\,\Omega$ coaxial probe through the ground plane. The width of an antenna array element is constrained by the element spacing, herein maintained at $\lambda/2$ @6 GHz to prevent grating lobes from occurring during beam steering up to 6 GHz. Fig. 1 depicts the CST Studio Suite unit-cell model of the proposed structure, including the optimized parameters such as the dimensions of the cavity, slot, Vivaldi taper length, and opening rate of the tapered slot [1].

2) Antenna Simulation: A unit cell with periodic boundary conditions in both the x- and y-directions is employed to

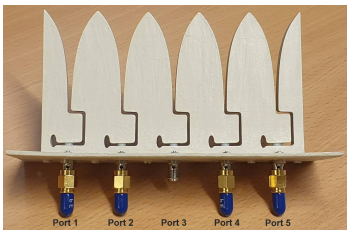

(a)

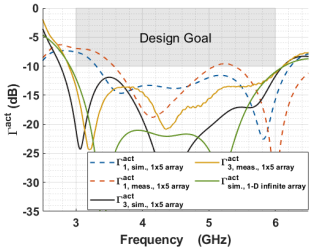

(b)

Fig. 3. (a) A 3D-printed 1×5 antenna array prototype after silver painting; (b) Simulated and measured active reflection coefficients at $\theta = 0$ and $\phi = 0$.

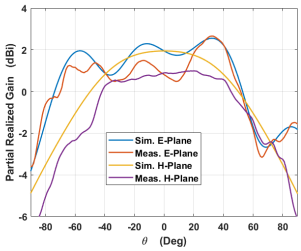

(a)

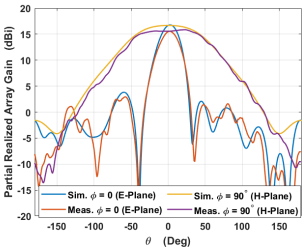

(b)

Fig. 4. Simulated and measured (a) embedded element pattern of the center element in the finite array and; (b) array antenna pattern for $\theta = 0°$ at 4.5 GHz in the E- and H-planes.

simulate and optimize the antenna element in a 2-D infinite array environment. The simulated active reflection coefficient Γ^{act} in the three elementary planes as a function of frequency and steering angle θ is shown in Fig. 2(a), and at 4.5 GHz for steering angles θ and ϕ in Fig. 2(b). Γ^{act} remains below -10 dB in the 3–6 GHz frequency range during scanning. Note that the symmetry of Γ^{act} persists in the grating lobe-free region, despite the feed-induced asymmetry in the elements [4]. However, slight variation Γ^{act} is observed due to re-meshing the structure and limited simulation accuracy.

The total realized embedded element gain can be directly calculated from Γ^{act} using [5]

$$G(\theta, \phi) = \frac{4\pi A}{\lambda^2} \cos(\theta)(1 - |\Gamma^{\text{act}}(\theta, \phi)|^2) \qquad (1)$$

where A denotes the physical aperture (unit cell) area of the radiating element. Hence, within the steering range where $|\Gamma^{\text{act}}| < -10$ dB, and without grating lobes, the active element pattern G is seen to closely approximate the $\cos(\theta)$ distribution. For our small-scale prototype array, however, uniformity and symmetry of the passive embedded element patterns are expected to degrade due to finite array edge effects, causing more centralized elements to behave differently from those near array edges.

III. Validation for 1-D Array

1) Manufacturing: The 3-D model of finite 1×5 array is printed using a Halot Mage 8K Resin 3D Printer. This printer has a $29.7\,\mu$m XY print resolution and is compatible with light-reactive thermoset materials. After the printing and curing process, the components undergo an initial cleaning phase. Subsequently, the water-based EMI silver Conductive Paint 842WB is applied with the help of a brush, resulting in several layers. Fig. 3(a) displays the 3D-printed, silver-coated 1×5 Vivaldi array with integrated coaxial probe connectors.

2) Comparison of Simulated and Measured Results: Fig. 3(b) displays the simulated and measured active reflection coefficient of the 1-st and 3-rd elements in the 1×5 Vivaldi array for the broadside scan angle[2]. Simulated and measured results closely match, and $|\Gamma^{\text{act}}| < -10$ dB across the entire frequency range.

[2]Although the antenna element was optimized in a 2-D infinite array, it was re-simulated in a 1-D infinite array to allow for a fair comparison.

Finally, the measured co-pol component of the radiation pattern of the center element closely aligns with the simulated results at the presented frequency, with a slight additional ripple in the measurements [*cf.* Fig. 4(a)]. As predicted, the co-pol patterns are not uniform due to the finite array size leading to edge effects. Fig. 4(b) illustrates a close alignment between the simulated and measured array antenna patterns for broadside scan. The radiation patterns show a slight deviation of ~ 1.2 dB primarily due to the dissipation loss from the silver coating. The simulated antenna radiation efficiency (η_{rad}) for the lossy coaxial-probe fed Vivaldi antenna employing real metals approaches 100%. However, η_{rad}[3] is determined by adjusting the simulation conductivity of the back-to-back feed structure to match the measured s_{21}. This so-fitted value is then used in the antenna simulation. The estimated η_{rad} surpasses 81% across the operational bandwidth.

IV. Conclusion

The 2-D Vivaldi antenna array elements operate in the 3–6 GHz frequency range and feature novel coaxial-probe-through-ground-plane feeds. The infinite array's active reflection coefficient remains below -10 dB for most of the steering and frequency range. Measured results from a small-scale 1×5 Vivaldi array align well with simulations, validating the infinite array model and probe feeding concept. The 3D printing and silver-coating fabrication process demonstrate effectiveness for rapid and cost-effective prototyping.

References

[1] H. Kähkönen, J. Ala-Laurinaho and V. Viikari, "Dual-Polarized Ka-Band Vivaldi Antenna Array," in IEEE Transactions on Antennas and Propagation, vol. 68, no. 4, pp. 2675-2683, April 2020.

[2] P. Benthem et al., "Aperture array development for future large radio telescopes," Proceedings of the 5th European Conference on Antennas and Propagation (EUCAP), Rome, Italy, 2011, pp. 2601-2605.

[3] M. I. M. Ghazali, K. Y. Park, J. A. Byford, J. Papapolymerou and P. Chahal, "3D printed metalized-polymer UWB high-gain Vivaldi antennas," 2016 IEEE MTT-S International Microwave Symposium (IMS), San Francisco, CA, USA, 2016, pp. 1-4.

[4] A. K. Bhattacharyya, "Active Element Pattern Symmetry for Asymmetrical Element Arrays," in IEEE Antennas and Wireless Propagation Letters, vol. 6, pp. 275-278, 2007.

[5] Craeye, C., and M. Arts (2004), "On the receiving cross section of an antenna in infinite linear and planar arrays," Radio Sci., 39, RS2010.

[3]$\eta_{\text{rad}} = \frac{P_{\text{rad}}}{P_{\text{rad}} + P_{\text{diss}}}$, where P_{diss} represents power loss due to the silver coating.